

Supplementary Information

Flow states of two dimensional active gels driven by external shear

Wan Luo^{*ab}, Aparna Baskaran^c, Robert A. Pelcovits^{de}, and Thomas R. Powers^{abde†}

* *Email: Wan_Luo@brown.edu*

† *Email: Thomas_Powers@brown.edu*

^a School of Engineering, Brown University, Providence, RI 02912, USA.

^b Center for Fluid Mechanics, Brown University, Providence, RI 02912, USA.

^c Martin Fisher School of Physics, Brandeis University, Waltham, MA 02453 USA.

^d Department of Physics, Brown University, Providence, RI 02912, USA.

^e Brown Theoretical Physics Center, Brown University, Providence, RI 02912, USA.

The supplementary information is divided into two sections: [S1](#) Straight channel and [S2](#) Annular channel. Movies of unsteady flow states in both the straight and annular channel cases are presented in this supplementary information. Also, more details about the contractile flows are shown, including the average flow rate, the wall stress in the straight channel case and the wall torque in the annular channel case. Additionally, we also show a comparison of simulation and weakly nonlinear analysis of zero shear rate case for the straight channel in the subsection [S1.5](#), and subsection [S2.4](#) shows linear analysis of the limit in which the flow in the annular channel is very slow.

S1 Straight channel

S1.1 Oscillatory flow state

A movie of the velocity field for positive spontaneous flow (Fig. 9a) is shown in the Movie S1: stra-posi-osci-U.gif. Note that in the title of the movie t is time in units of τ , a is activity in units of $\eta/(\tau\lambda)$, and u_0 is moving velocity of the bottom plate of the straight channel (i.e. $\dot{\gamma}W$ in the main text) in units of W/τ . The director and scalar order parameter fields for positive spontaneous flow (Fig. 9b) are shown in the Movie S2: stra-posi-osci-Q.gif. The velocity field for negative spontaneous flow (Fig. 9c) is shown in the Movie S3: stra-negt-osci-U.gif. The director and scalar order parameter fields for negative spontaneous flow (Fig. 9d) are shown in the Movie S4: stra-negt-osci-Q.gif.

S1.2 Oscillatory-like flow state

An example of a dynamical final state for oscillatory-like flow with $\dot{\gamma} = 0$ and $\alpha = 2.3$. The flow pattern is not perfectly periodic in the horizontal direction. A movie of the velocity field is shown in the Movie S5: stra-oscilike-U.gif. A movie of the director and scalar order parameter fields is shown in the Movie S6: stra-oscilike-Q.gif.

S1.3 Dancing flow state

Movies for the example of the dancing flow state shown in Fig. 10. A movie of the velocity field is shown in the Movie S7: stra-danc-U.gif. A movie of the director and scalar order parameter fields is shown in the Movie S8: stra-danc-Q.gif.

S1.4 Flow rate and wall stress of contractile fluids

The steady-state of activity-driven volumetric flow rate and average wall stress imposed by the active flow on the bottom plates of the channel for contractile fluids.

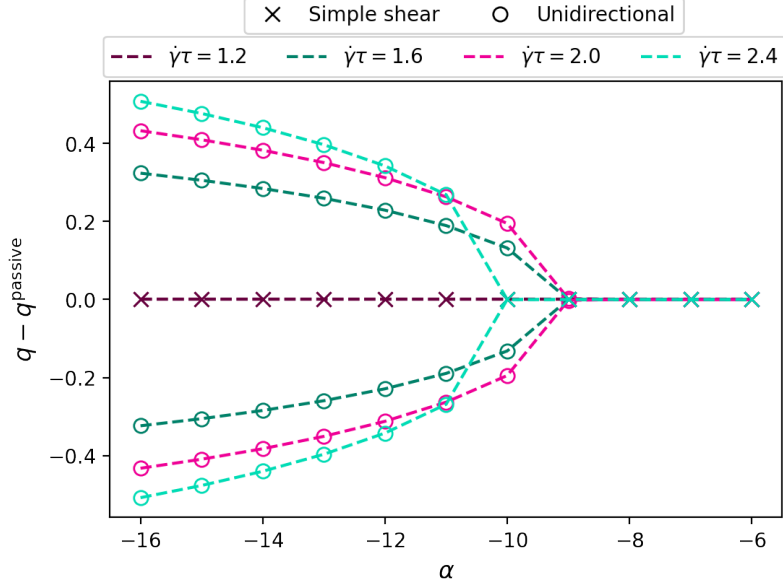


Figure S1: Activity-driven volumetric flow rate in contractile fluids in the straight channel. Symbols denote the flow state and colors denote the external shear rates. The plot shows results for the two kinds of initial conditions of the director field with a positive and negative x component.

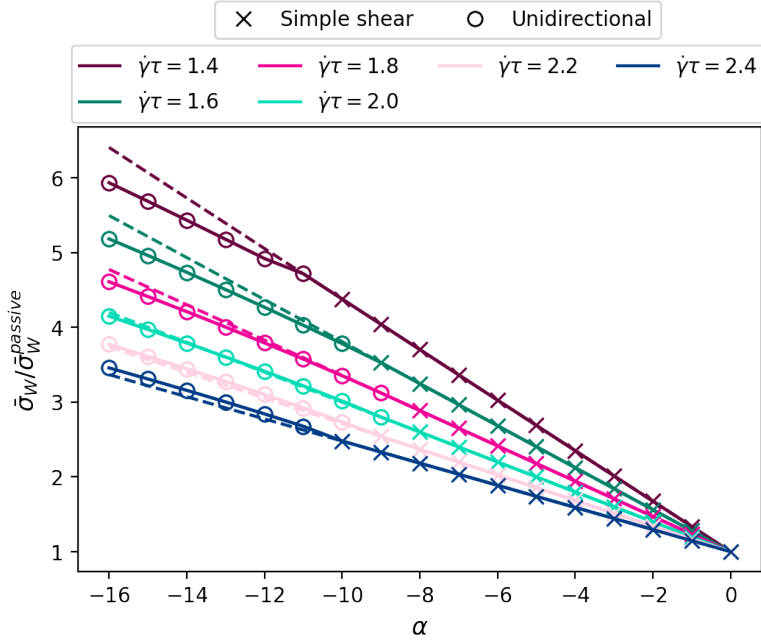


Figure S2: The average wall stress imposed by the active flow on the bottom plates of the straight channel $\bar{\sigma}_W$ as a function of dimensionless activity α for contractile fluids. The dashed lines are extended lines of simple shear flow. They are plotted for comparing the different slopes of simple shear flow and unidirectional flows. The results in the figure are insensitive to the two kinds of initial conditions for the director field, i.e., $\pm x$ splay-like alignment.

S1.5 Comparison of simulation and weakly nonlinear analysis of zero shear rate case

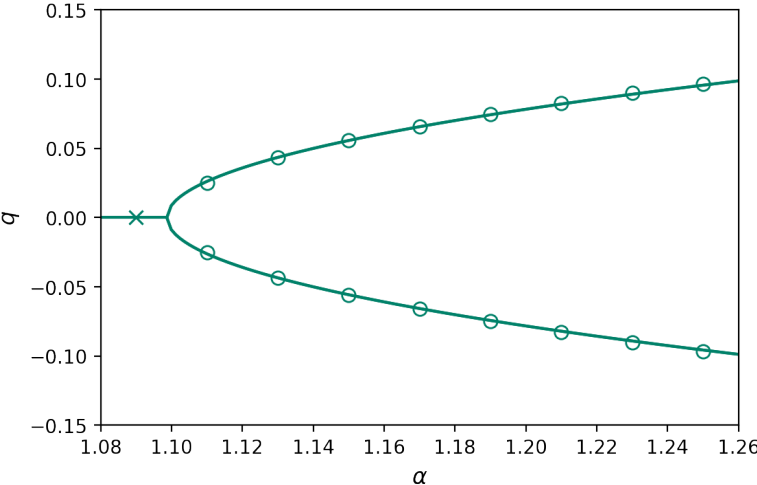


Figure S3: The flux of the flows near the critical activity. Lines denote the results from weakly nonlinear analysis. Symbols denote the finite element results.

Two results match each other well for the case when there is no external shear rate and activity is just above the the critical activity.

S2 Annular channel

S2.1 Oscillatory flow state

A movie of the velocity field for positive spontaneous flow (Fig. 15e) is shown in the Movie S9: annu-osci-U.gif. Note that in the title of the movie t is time in units of τ , a is activity in units of $\eta/(\tau\lambda)$, and ω is rotation frequency of the inner boundary of the annular channel in units of $1/\tau$. The director and scalar order parameter fields for positive spontaneous flow (Fig. 15f) are shown in the Movie S10: annu-osci-Q.gif.

S2.2 Dancing flow state

A movie of the velocity field of the dancing flow state (Fig. 15g) is shown in the Movie S11: annu-danc-U.gif. Director and scalar order parameter fields of the dancing flow state (Fig. 15h) are shown in the Movie S12: annu-danc-Q.gif.

S2.3 Flow rate and wall torque of contractile fluids

Steady-state of activity-driven volumetric flow rate and wall torque imposed by the active flow on the inner disk of the annular channel in contractile fluids.

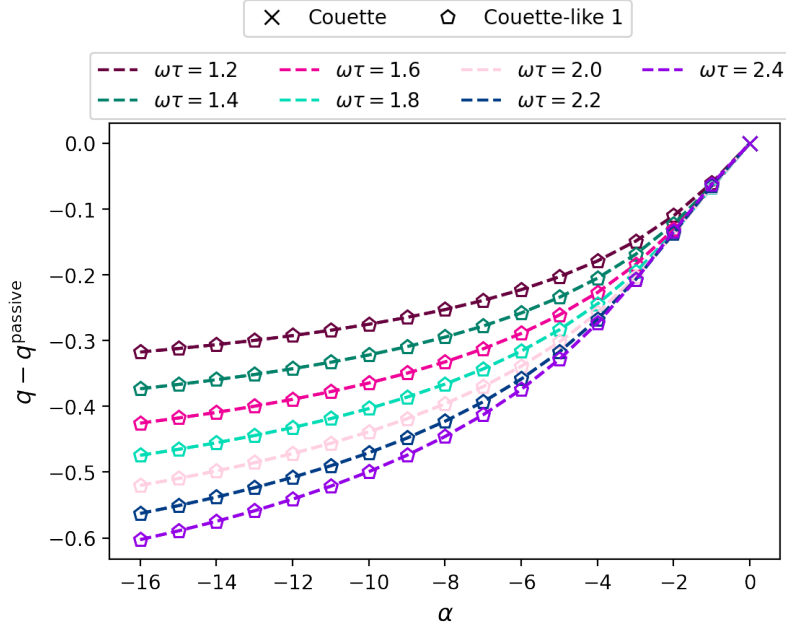


Figure S4: Activity-induced flux for contractile fluids in dimensionless units of $v_{\theta}\tau/W$ as a function of activity in the annular channel. The plot shows results for the two kinds of initial conditions of the director field with a positive and negative θ component.

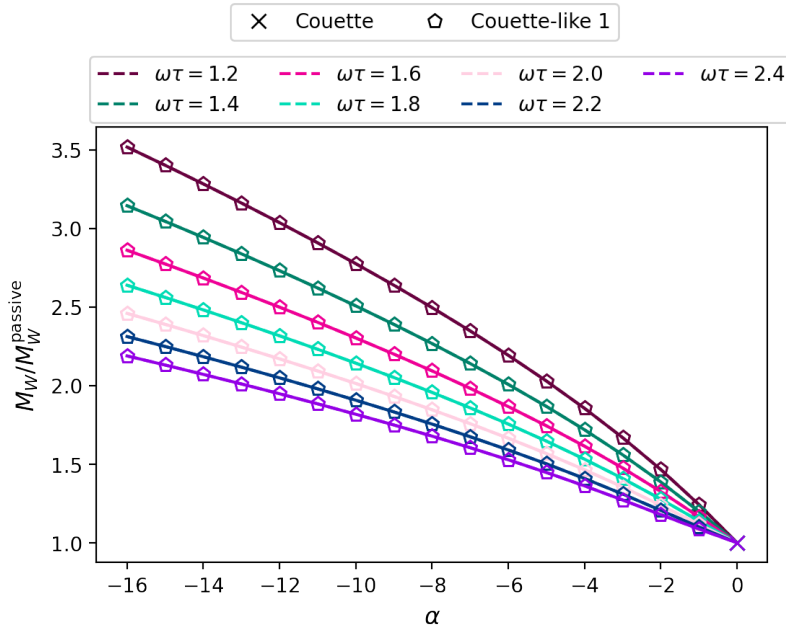


Figure S5: The wall torque of different active flows normalized by the passive flow in contractile fluids in the annular channel. The results in the figure are insensitive to the two kinds of initial conditions for the director field, i.e., clockwise and counterclockwise splay-like alignment.

S2.4 Annular channel: Linear analysis of curvature at low shear rate

In this section we study the limit in which the flow in the annular channel is slow enough that the induced order is small, $S \ll 1$. For slow enough flow, it is valid to neglect the nonlinear terms in eqn (4). On the one hand, this analysis offers a theoretical explanation of some of the observations in Sec. 5; on the other hand, it gives some insight into the role of the curvature of the boundaries, which we did not vary in the Sec. 5. For convenience, here we restate the modified Stokes equation (eqn (3)) in dimensionless form, along with the dimensionless form of the steady linearized equation for \mathbf{Q} :

$$0 = -\nabla p + \nabla^2 \mathbf{v} - \frac{\alpha}{\lambda} \nabla \cdot \mathbf{Q} \quad (\text{S1})$$

$$0 = -\mathbf{Q} + \ell^2 \nabla^2 \mathbf{Q} + 2\lambda \mathbf{E}, \quad (\text{S2})$$

As in our numerical calculations, we use the width W of the channel as the unit of length. Since we seek to study the Couette-like flow state, we assume $\mathbf{v} = v_\theta(r)\hat{\boldsymbol{\theta}}$. Note that this flow is incompressible. We also suppose that p , Q_{rr} , and $Q_{r\theta}$ are functions of radius only. With these assumptions, the rr component of eqn (S2) is homogeneous, which together with the Neumann boundary conditions $\partial_r Q_{rr} = 0$ at $r = R/W$ and $r = R/W + 1$ implies $Q_{rr} = 0$. Since the radial component of the modified Stokes equation (eqn (S1) with $Q_{rr} = 0$) implies that the pressure gradient vanishes, we take $p = 0$.

To solve for the velocity and order parameter fields, we take the divergence of eqn (S2) and combine

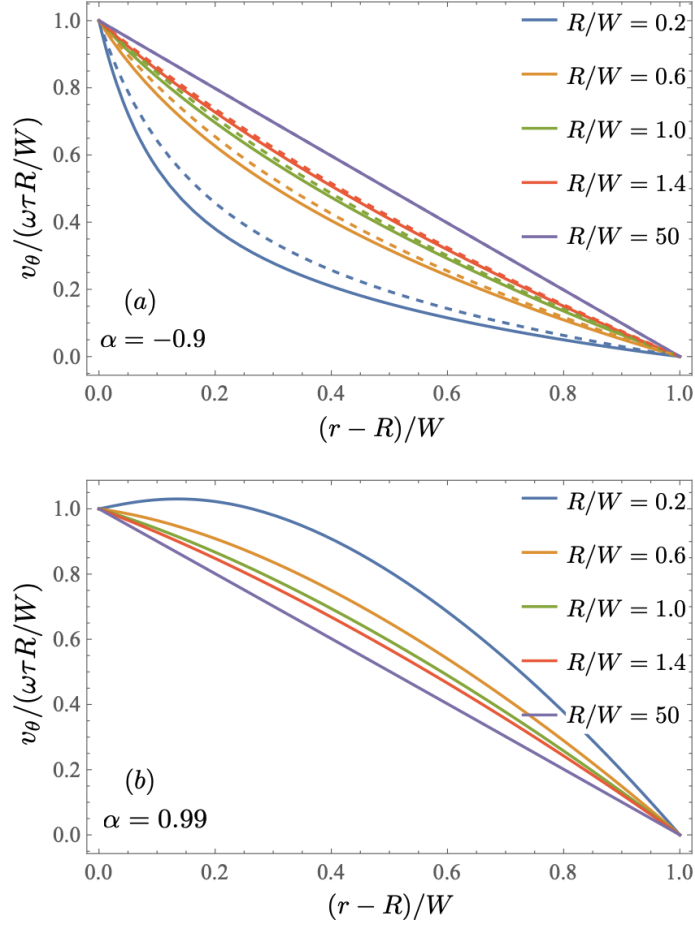


Figure S6: Analytical results for flow velocity of the Couette-like 1 state in an annular channel with weak order for $\ell = 0.1$, $\lambda = 1$, and various values of R/W for (a) a contractile fluid with $\alpha = -0.9$ and (b) an extensile fluid with $\alpha = 0.99$. The dashed lines in the panel (a) show the results for Newtonian flows ($\alpha = 0$) for comparison.

with eqn (S1) with $p = 0$ to find

$$\nabla^2 \left(\nabla^2 - \frac{1}{\xi^2} \right) \mathbf{v} = 0, \quad (\text{S3})$$

where $\xi^2 = \ell^2 / (1 - \alpha)$. To focus our attention on the Couette-like states only, we restrict our analysis to $\alpha < 1$ in this section. Thus,

$$v_\theta = c_1 r + c_2 / r + c_3 I_1(r/\xi) + c_4 K_1(r/\xi), \quad (\text{S4})$$

where the c_i are constants to be determined, and $I_1(x)$ and $K_1(x)$ are modified Bessel functions. Inserting the velocity field eqn (S4) into the $r\theta$ component of eqn (S2),

$$0 = \ell^2 \left(Q''_{r\theta} + \frac{1}{r} Q'_{r\theta} - \frac{4}{r^2} Q_{r\theta} \right) - Q_{r\theta} + \lambda \left(v'_\theta - \frac{v_\theta}{r} \right), \quad (\text{S5})$$

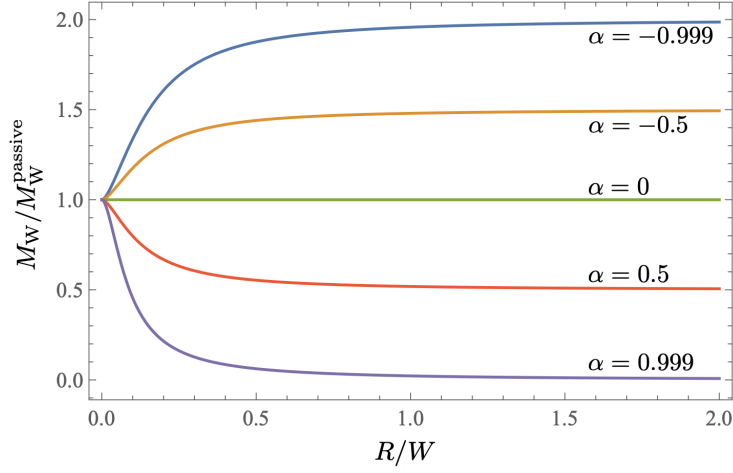


Figure S7: Dependence of normalized wall torque on R/W for different α from linear analysis at low shear with $\ell = 0.1$ and $\lambda = 1$. The colors denote different activities.

yields

$$\begin{aligned} & \ell^2 \left(Q''_{r\theta} + \frac{1}{r} Q'_{r\theta} - \frac{4}{r^2} Q_{r\theta} \right) - Q_{r\theta} \\ &= \frac{\lambda}{\xi} \left[\frac{2c_2\xi}{r^2} - c_3 I_2(r/\xi) + c_4 K_2(r/\xi) \right], \end{aligned} \quad (\text{S6})$$

which has general solution

$$\begin{aligned} Q_{r\theta} &= c_5 I_2(r/\ell) + c_6 K_2(r/\ell) - 2c_2\lambda/r^2 \\ &- c_3 \frac{\lambda\xi}{\ell^2 - \xi^2} I_2(r/\xi) + c_4 \frac{\lambda\xi}{\ell^2 - \xi^2} K_2(r/\xi). \end{aligned} \quad (\text{S7})$$

Inserting this solution into the modified Stokes equation [eqn (S1)] shows that $c_5 = c_6 = 0$. The rest of the integration constants are determined by the no-slip boundary conditions on the (dimensionless) velocity, $v_\theta(R/W) = \omega\tau R/W$ and $v_\theta(R/W + 1) = 0$, and the Neumann boundary conditions on the order parameter field $Q'_{rr}(R/W) = Q'_{rr}(R/W + 1) = 0$. The complete formulas are too complicated to display, but we plot the velocity in Fig. S6 for various ratios of R/W for a representative contractile case (top panel) and extensile case (bottom panel). In both cases, the flow velocity approaches a linear profile as R/W becomes large, as expected, since in that limit the curvature of the annulus becomes unimportant, and the flow approaches simple shear flow. For the contractile case, Fig. S6a, the velocity profile is close to the Newtonian result, with the agreement between the two cases getting better as R/W increases. For the extensile case, the velocity curves for different values of R/W get closer to each other as α increases, becoming very close to the linear profile around $\alpha = 0.885$. Above this value of activity, the order of the curves reverses, with the linear curve lying below all the other curves. When α gets very close to unity and R/W is small, the maximum velocity is not at the wall, i.e. the flow continuously changes from the Couette-like 1 state to the Couette-like 2 state [Fig. S6b]. Fig. S7 shows the total torque $M = 2\pi R^2 \sigma_{r\theta}$ on the circle $r = R$ as a function of R/W . Note that

the limit of a straight channel is almost obtained when R becomes comparable to W . The torque for a contractile fluid is higher than the passive value since contractile fluids effectively increase the shear viscosity. Likewise, the torque for an extensile fluid is less than the passive value. The torque approaches the passive value when $R \ll W$. Note that since we use W as the unit of length, the limit $R \ll W$ corresponds to making the inner cylinder of vanishing thickness. When $R < \ell$, the term $\ell^2 \nabla^2 \mathbf{Q}$ dominates eqn (S2), and therefore $\mathbf{Q} \rightarrow 0$. In this limit, the active force vanishes, and flow is Couette flow.

It is informative to find the velocity and the order parameter field in the limit $R \gg W$, where the curvature of the annulus is small. Rather than taking the limit of the formulas used to make Figs. S6 and S7, it is simplest to solve the equations directly using regular perturbation theory in powers of W/R . Reinstating the dimensions and writing $r = R + y$, we find

$$v_\theta = \omega R \left(1 - \frac{y}{W}\right) - \frac{\omega y}{2} \left(1 - \frac{y}{W}\right) + \frac{2\alpha\ell^2\omega W}{1-\alpha} \left[\frac{1 - \cosh[(1-2y/W)/\xi]}{\cosh[1/(2\xi)]} \right] \quad (\text{S8})$$

$$Q_{r\theta} = -\frac{\lambda\omega\tau R}{W} + \frac{\lambda\omega\tau}{2} \left[4y/W - 3 + 4\xi \frac{\sinh[(1-2y/W)/\xi]}{\cosh[1/(2\xi)]} \right]. \quad (\text{S9})$$

The first terms of eqns (S8) and (S9) correspond to the velocity and order parameter field, respectively, of a straight channel with an infinitesimal imposed shear rate $\dot{\gamma} = \omega R/W$. The remaining terms are the corrections due to the nonzero curvature of the annular channel. Unlike our weakly analysis of the active flow in the straight channel (Sec. 4.3), which had spontaneous flow in either direction, here we see that the component of flow driven by the activity has a definite sign, and is the same direction as externally imposed flow for extensile fluids.